Analytical heat transfer analysis for CMS support infrastructure in the Phase-2 Upgrade

J A Knox[1], Dr. Andromachi Tsioru[2]

[1]Department of Engineering Mathematics, University of Bristol, United Kingdom
[2]CERN, Switzerland

Keywords: Heat transfer, Barrel Tracker Support Tube, heater foils, analytical modelling, thermal analysis

Abstract

This report presents an analytical modelling approach to estimate heat transfer across the Compact Muon Solenoid (CMS) subdetectors at the High-Luminosity Large Hadron Collider (HL-LHC). A thermal screen isolates the subdetectors at their respective operating temperatures, with active thermal control provided by an array of heater foil elements. The required power generation from the array is dependent on the heat flux at the outer surface of the Barrel Tracker Support Tube (BTST). A reduced order analysis was performed to estimate the heat flux in this location, with empirical and analytical models used to approximate the thermal behaviour of the BTST core. Including a 30% safety factor, empirical estimations exceed analytical counterparts by 13% and predict a maximum heat flux of 92 W/m^2. Previous approximations suggest 123 W/m^2 is suitable. The accuracy of empirical modelling results remains uncertain until test specifics are acquired from the core manufacturer. Minimal gas dependency is shown over the operating conditions.

Introduction

The High Luminosity Large Hadron Collider (HL-LHC) is an upgrade to the existing LHC which seeks to increase the instantaneous peak luminosity (rate of collisions) by a factor of five and the integrated luminosity (total number of collisions) by a factor of ten beyond the original design value [1]. This advancement may enable experiments to expand the size of collision event datasets by one order of magnitude relative to the LHC baseline. However, the increase in radiation associated with higher luminosity requires detectors with enhanced radiotolerance, improved granularity, and greater bandwidth to accommodate higher data rates [2]. The Compact Muon Solenoid (CMS) detector at the LHC is currently replacing or upgrading most of its subdetectors under the Phase-2 upgrade programme (Ph-2) in preparation for operations at the HL-LHC. A thermal screen will isolate several subdetectors, which function at very different temperatures and in close proximity. The thermal screen may be realised as a thin cylindrical shell whose internal and external lateral surfaces are actively regulated, such that heat flux and temperature constraints may be imposed. An array of resistive heater foils positioned on the external surface provides a variable heat flux, while the internal surface is regulated with an isothermal cold plate. Heat transfer analysis across infrastructure contained within the thermal screen is therefore necessary to determine the requisite power generation of the heater foil array. This report aims to verify the expected heat transfer across support infrastructure within the thermal screen using a one-dimensional analytical modelling approach.

Background

The Barrel Tracker Support Tube (BTST) is a hollow cylindrical support structure housing the Barrel Timing Layer (BTL) and Barrel Tracker (BT) subdetectors, which operate between $-25°C$ and $-40°C$ to minimise radiation damage to sensitive silicon components. Figure 1 provides a cross-sectional view of the inner detector subassembly. The electromagnetic calorimeter (ECAL) is positioned externally to the BTST and encloses the subassembly described above with a clearance of approximately 2mm. The

ECAL barrel layer contains avalanche photodiodes for particle detection, and two endcaps seal the structure. Operational temperatures in the barrel layer are to decrease from 18°C to 9°C under Ph-2 to reduce avalanche photodiode noise [2]. Due to the substantial variance in operational temperatures between ECAL and the BTL, significant heat transfer is expected across the structures.

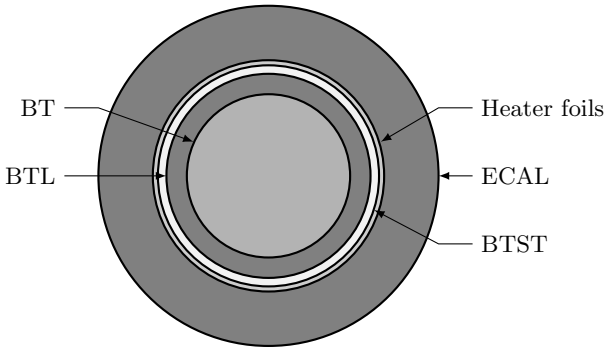

Figure 1: Schematic cross-section of inner CMS subdetectors. ECAL endcaps not shown.

Thermal Screen Description

A schematic cross-section of the thermal screen is presented in Figure 2. A cold plate within the BTL maintains a constant temperature of −35°C and defines the inner surface of the thermal screen. A gas chamber with an annular width of 2 mm houses control systems electronics. Any heat generated by the electronics is assumed to be dissipated by an isolated convective cooling system. The thermal mass and volume of the electronics is also assumed negligible, such that annular natural convection may be approximated in the chamber. The subdetectors may be saturated with either dry air or nitrogen gas, depending on the state of operation. An Airex® foam of 6 mm thickness insulates the subdetector interface, bonded with 0.2 mm resin. An array of resistive heater foil circuits affixed to the external surface of the BTST defines the outer surface of the thermal screen. The array must maintain a surface temperature between 9°C and 13°C. The BTST comprises two 2 mm thick facesheets enclosing a 26 mm thick honeycomb core. The core structure has a density of 64 kg/m^3 and is manufactured from Nomex® paper dipped in phenolic resin, otherwise referred to as the foil. The core consists of 3.2 mm non-corrugated hexagonal cells with 0.1 mm foil thickness. The facesheets are composed of HM63 carbon fiber impregnated with PMT-F6 resin and are bonded to the core using Araldite® 2011 epoxy adhesive film with an estimated thickness of 0.1 mm.

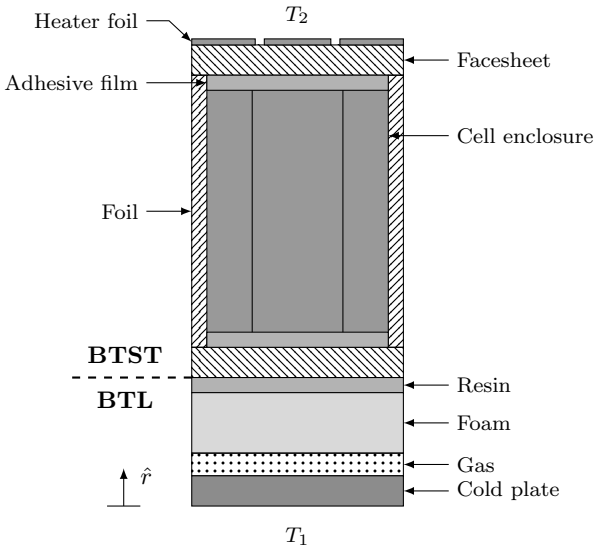

Figure 2: Schematic cross-section of the thermal screen, where $\hat{r}$ is the positive radial direction.

Heat Transfer Analysis

A reduced order modelling approach was adopted to estimate the heat flux at the outer surface of the thermal screen. Conduction and radiation are regarded as the principal modes of heat transfer in this study, substantiated by the following analysis. Hollands studied natural convection in horizontal thin-walled honeycomb panels and determined the critical Rayleigh number for the onset of natural convection in square cells [3]. The maximum Rayleigh number calculated for the honeycomb core used in this work was approximately $1.6 \cdot 10^5$, in comparison to the critical Rayleigh number of $8.6 \cdot 10^6$ for equivalent geometry. Similar arguments are asserted for the gas chamber. Assuming the annular enclosure may be approximated by an infinite horizontal layer with rigid (no-slip) and isothermal top and bottom boundaries,

it can be shown that the convection onset criterion is not met (for small temperature differences) [4, 5]. Thus, the heat transfer rate across the quiescent fluid layer is well-approximated by pure conduction.

The Fourier-Biot equation was formulated in polar coordinates and applied to a hollow cylindrical volume approximating the thermal screen, as seen in Figure 3a. For the purposes of simplifying analysis, the temperature distribution was assumed to be uniform in the axial and azimuthal directions. This assumption reduced the problem to a one-dimensional case. The bulk material was assumed to be isotropic and homogeneous, with no internal heat generation. Given a steady-state problem, the governing partial differential equation reduces to:

$$\frac{\partial}{\partial r}\left(r\frac{\partial T}{\partial r}\right) = 0 \tag{1}$$

where r is the radial coordinate and T is temperature. Isothermal boundary conditions were assumed at the inner and outer lateral surfaces:

$$T(r_i) = T_i, \quad i = 1, 2 \tag{2}$$

After solving (1) for the temperature distribution using the boundary conditions, it follows from Fourier's law that the heat transfer rate $\dot{Q}$ is:

$$\dot{Q} = \frac{\Delta T}{R} \tag{3}$$

where ΔT is the driving force and R is thermal resistance to heat transfer, given by:

$$R = \frac{r_2 - r_1}{kA_{lm}} \tag{4}$$

where k is the thermal conductivity of the bulk material evaluated at the arithmetic mean of the driving force and A_{lm} is the logarithmic mean area. For composite cylinders, assuming perfect thermal contact between interfaces, since the total heat transfer rate in any radial plane is constant, $\dot{Q}$ may be expressed in terms of the respective thermal resistances of each layer:

$$\dot{Q} = \frac{\Delta T}{\sum\limits_j R_j}, \quad j = 1, ..., n \tag{5}$$

where the j index refers to a given layer within the cylindrical structure. The heat transfer rate across the thermal screen may therefore be characterised in terms of $(n = 8)$ thermal resistances, as the cold plate represents a boundary condition. Figure 3b presents a diagram of the composite system. It remains to determine the thermal resistances of each layer, contingent upon first resolving the respective thermal conductivities. For the insulating foam and resin, this is trivial. The thermal conductivity of gas layer is temperature-dependant and should be evaluated at the temperature of the cold plate, since minimal heat transfer is expected across the chamber. Since the facesheets exhibit anisotropic thermal behaviour, the rule of mixtures may be used to estimate the effective thermal conductivity in the radial direction [6]:

$$k_{fs} = k_m \frac{k_{fb}(1 + V_{fb}) + k_m(1 - V_{fb})}{k_{fb}(1 - V_{fb}) + k_m(1 + V_{fb})} \tag{6}$$

where k_{fs} is the effective thermal conductivity of the facesheet, V_{fb} is the volume fraction of the fibre and k_{fb} and k_m are the thermal conductivities of the fibre and matrix respectively. The following sections present potential modelling strategies to estimate the equivalent thermal conductivity of the BTST core.

Swann-Pittman Model

The semi-empirical Swann-Pittman (SP) model for heat transfer through honeycomb core structures is reported as the standard for aerospace industry applications [7, 8]. Facesheet thickness is assumed small, such that thermal contributions are negligible. Cell cross sections are assumed circular. A parallel thermal network was developed to model solid and gas conduction in the core, superimposed with an empirical relationship describing radiation in the core enclosure. The effective thermal conductivity k_e is given by:

$$k_e = k_f \frac{\Delta A}{A} + k_g\left(1 - \frac{\Delta A}{A}\right) + k_r \tag{7}$$

where k_f is the thermal conductivity of the foil material, k_g is the thermal conductivity of the gas saturating the panel, $\Delta A/A$ is the ratio of cross sectional areas of the solid core to the overall cell and k_r

is the radiation effective thermal conductivity, given by:

$$k_r = 0.664(\lambda + 0.3)^{-0.69}\epsilon^{1.63(\lambda+1)^{-0.89}} L'\sigma(T_1 + T_2)(T_1^2 + T_2^2) \tag{8}$$

where σ is the Stefan-Boltzmann radiation constant, L' is the thickness of the gas column in the cell, T_1 and T_2 are the temperatures of the facesheets, λ is the ratio of cell height to cell diameter and ϵ is emissivity. The facesheets and foil are assumed to have the same emissivity. The area ratio $\Delta A/A$ may be identified using the mass density ratio of the honeycomb core to the bulk material. The equivalent diameter of the hexagonal cells may be obtained by equating the perimeters of the hexagonal and circular cross sections, as suggested by Swann and Pittman [9]. However, the thermal effects of adhesive bonding are not accounted for.

Modified Swann-Pittman Model

The Modified Swann-Pittman model (MSP), proposed by [7], integrates the effects of the facesheets and adhesive directly into the SP model. The modified equivalent thermal network appends four thermal resistances arranged in series. Two resistances account for solid conduction through the facesheets, and two describe the parallel arrangement of solid conduction through the adhesive and segment of foil covered by the adhesive. The overall effective thermal conductivity from the MSP model is defined by:

$$\frac{L}{k_e} = \frac{2L_{fs}}{k_{fs}} + \frac{2L_{ad}}{k_f\frac{\Delta A}{A} + k_{ad}\left(1 - \frac{\Delta A}{A}\right)} + \frac{L'}{k_f\frac{\Delta A}{A} + k_g\left(1 - \frac{\Delta A}{A}\right) + k_r} \tag{9}$$

where L, L_{fs} and L_{ad} are the thicknesses of the overall panel, facesheet and adhesive respectively, and k_{ad} is the thermal conductivity of the adhesive.

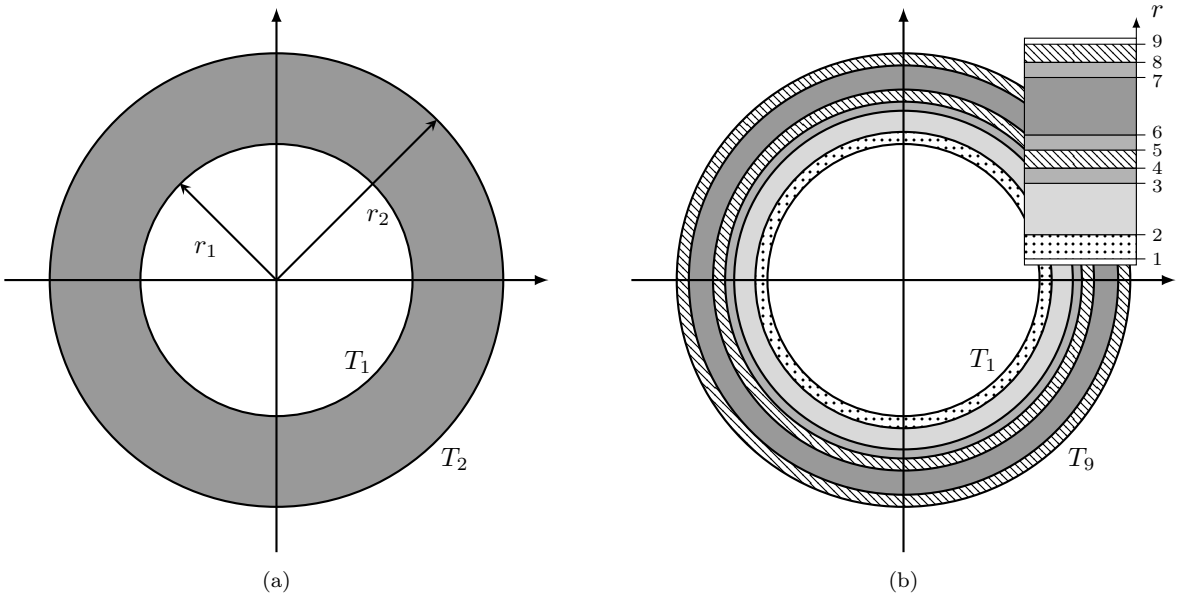

Figure 3: (a) Single layer approximation and (b) composite representation of the thermal screen. Zoomed view shows the radial index of each layer.

Hence, the thermal resistance of the entire BTST may be effectively characterised by the MSP equivalent thermal conductivity. In cases where the emissivity of the adhesive and foil layers differ, a weighted emittance based on the ratio of the surface area of each material to the total surface area involved in the radiation exchange in the enclosure may be used.

Empirical Model

HexCel, the manufacturer of the BTST core, report to have tested several honeycomb cores in order to characterise thermal conductivity [10]. Details of such tests are not provided in the reference and an assessment of thermal conductivity via numerical analysis or experiment is highly recommended. Given the core geometry, the effective thermal conductivity estimated by HexCel is $k_e = 0.45$ W/mK. Note, this value was obtained through application of heat flow from top to bottom of the panel (opposing the natural direction of buoyancy). The heat transfer path will differ from this configuration around the circumference of the thermal screen.

Results and Discussion

Figure 4 compares the thermal conductivity of dry air and nitrogen gas over the range of temperatures expected within the thermal screen. Across the temperatures studied, the thermal conductivity of dry air consistently exceeds that of nitrogen gas by an average of 0.3 mW/mK. Therefore, although dry air models represent the upper limit of heat transfer across the thermal screen, the difference in the results is expected to be marginal. Since the only available empirical data for the equivalent thermal conductivity of the core was obtained in the presence of air, all subsequent results assume core saturation with the same gas. Figure 5 shows heat flux with respect to temperature at the outer surface of the thermal screen. Each model is identical in all aspects except for the BTST core layer, which designates the model type. Minimal variation in the results is observed between the SP and MSP models, attributed to the limited thermal impact of the adhesive layer. This contribution may be disregarded in subsequent modelling efforts.

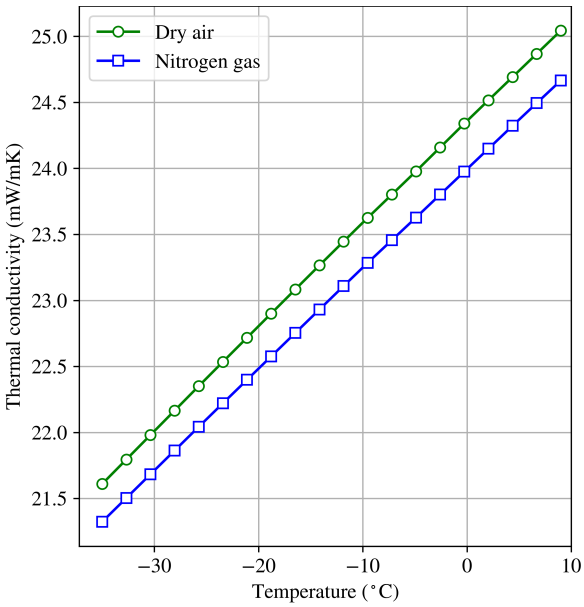

Figure 4: Plot thermal conductivity for dry air and nitrogen over the expected operating temperatures within the thermal screen.

The empirical model, on average, estimates the required heat flux as 13% higher than SP variants across the temperature range studied. Note, the effective thermal conductivity of the honeycomb core was obtained for heat flow from top to bottom of a horizontal panel. Analytical models assume a similar configuration. This geometry is only valid in the upper local region of the thermal screen. Variations in effective core thermal conductivity, which significantly impacts the overall resistance to heat transfer, are likely around the circumference of the structure. For instance, heat transfer may increase at the bottom of the structure where thermal gradients are aligned with the direction of natural buoyancy. Arguments concerning model discrepancy should be deferred until further details of the empirical tests are established, as thermal gradients and absolute test temperatures may influence conduction and the onset of natural convection within the panel. Contact with the manufacturer is highly advised. Incorporating a safety factor of 30%, the upper estimate of heat flux required at the outer surface of the BTST is 92 W/m^2.

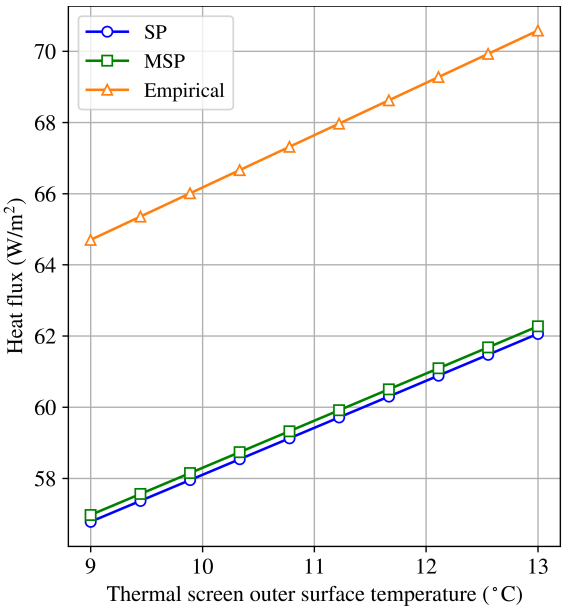

Figure 5: Plot of heat flux versus thermal screen outer surface temperature.

Adjusting power requirements from the existing Tracker subdetector indicates a necessary heat flux of 123 W/m^2, including the safety factor [11]. However, due to differences in the infrastructure between the current subassembly and the Ph-2 upgrade, inaccuracies in this estimate are expected.

Given the modular construction of infrastructure within the thermal screen, localised temperature peaks may occur at interfaces between the components. This thermal characteristic cannot be easily described using an analytical modelling approach. Therefore, while the average power of the heater foil array may be estimated, numerical simulation is necessary to determine non-uniform power distribution.

Conclusions

This report examined the steady state heat transfer across CMS infrastructure at the High Luminosity Large Hadron Collider (HL-LHC) over a range of operating temperatures. A one-dimensional model was developed to estimate the average heat flux required from a heater foil array positioned at the outer surface of the Barrel Tracker Support Tube (BTST). Within this framework, several component models were proposed to identify the effective thermal conductivity of complex core structures. The empirical estimation of heat flux exceeded that of analytical counterparts by 13%, establishing an upper limit of 92 W/m^2. However, the validity of the models is confined to a small local region, and variation in the heat flux is expected around the circumference of the structure. Conclusions about model discrepancy cannot be drawn until test details are confirmed with the core manufacturer. Minimal variation in the results is expected when the subassembly is saturated with dry air or nitrogen gas, due to similar thermal conductivities over the temperature range. Numerical simulation work is required to capture complex thermal behaviour in higher dimensions, such as non-uniform temperature peaks.

References

[1] I. Béjar Alonso et al. *High-Luminosity Large Hadron Collider (HL-LHC): Technical design report*. Tech. rep. 2020. DOI: https://doi.org/10.23731/CYRM-2020-0010.

[2] K. Klein et al. *The Phase-2 Upgrade of the CMS Tracker - Technical Design Report*. Tech. rep. CERN, 2017.

[3] K. G. T. Hollands. ""Natural Convection in Horizontal Thin-Walled Honeycomb Panels"". In: *Journal of Heat Transfer* 95.4 (Nov. 1973), pp. 439–444. ISSN: 0022-1481. DOI: https://doi.org/10.1115/1.3450086.

[4] Adrian Bejan. *Convection Heat Transfer*. John Wiley & Sons, Inc., 2013, pp. 263–264.

[5] M. Fossa et al. *Thermo-hydraulic design of the thermal screen of the CMS Tracker*. Tech. rep. Apr. 1999.

[6] George Voyiadjis et al. *Mechanics of Composite Materials with MATLAB*. Springer, 2005.

[7] Kamran Daryabeigi. *Heat Transfer in Adhesively Bonded Honeycomb Core Panels*. Tech. rep. Sept. 2001.

[8] Chupeng He et al. "Numerical Simulation of the Out-of-Plane Equivalent Thermal Conductivity of Honeycomb Core". In: *2020 International Conference on Artificial Intelligence and Electromechanical Automation (AIEA)*. 2020, pp. 854–857. DOI: 10.1109/AIEA51086.2020.00185.

[9] R.T. Swann et al. *Analysis of Effective Thermal Conductivities of Honeycomb Core and Corrugated-Core Sandwich Panels*. Tech. rep. Apr. 1961.

[10] HexCel. *HexWeb HRH-10 Aramid Fibre/Phenolic Honeycomb Product Data*. Jan. 2013.

[11] Nicola Bacchetta. *BTST Heating Foils Integration Aspects*. CERN. June 2023.